Journal of Power Sources 190 (2009) 336–340

Contents lists available at ScienceDirect

Journal of Power Sources

journal homepage: www.elsevier.com/locate/jpowsour

Short communication

Electrochemical impedance studies of electrooxidation of methanol and formic acid on Pt/C catalyst in acid medium

Zhen-Bo Wang*, Yuan-Yuan Chu, Ai-Fen Shao, Peng-Jian Zuo, Ge-Ping Yin

School of Chemical Engineering and Technology, Harbin Institute of Technology, No. 92 West Da-Zhi Street, Harbin 150001, China

ARTICLE INFO

Article history:
Received 8 December 2008
Received in revised form 3 January 2009
Accepted 7 January 2009
Available online 19 January 2009

Keywords:
Electrochemical impedance
Pt/C catalyst
Methanol electrooxidation
Formic acid electrooxidation

ABSTRACT

Cyclic voltammetry (CV), amperometric $i-t$ experiments, and electrochemical impedance spectroscopy (EIS) measurements were carried out by using glassy carbon disk electrode covered with the Pt/C catalyst powder in solutions of 0.5 mol L^{-1} H_2SO_4 containing 0.5 mol L^{-1} CH_3OH and 0.5 mol L^{-1} H_2SO_4 containing 0.5 mol L^{-1} HCOOH at 25 °C, respectively. Electrochemical measurements show that the activity of Pt/C for formic acid electrooxidation is prominently higher than for methanol electrooxidation. EIS information also discloses that the electrooxidation of methanol and formic acid on the Pt/C catalyst at various polarization potentials show different impedance behaviors. The mechanisms and the rate-determining steps of formic acid electrooxidation are also changed with the increase of the potential. Simultaneously, the effects of the electrode potentials on the impedance patterns were revealed.

1. Introduction

In the past decades, most of the research in fuel cell field is focused on direct methanol fuel cell (DMFC). However, two major disadvantages of DMFC, namely the high methanol crossover from anode to cathode through the polymer proton exchange membrane and the low activity of catalyst, prevent it from making broad commercial applications [1–4]. Research indicated that the formic acid crossover could be reduced by five times in comparison with methanol under the same conditions due to the repulsive interaction between the anions and membrane sulfonic groups as it partially dissociates in water and forms an anion ($HCOO^-$), and a higher performance of direct formic acid fuel cell (DFAFC) can be obtained [4,5]. A decrease of fuel crossover will improve the overall cell efficiency, and allow the use of high concentrations of formic acid, which can also facilitate water management [6]. In addition, formic acid has a higher theoretical open circuit potential (1.45 V) calculated from the Gibbs free energy than methanol and is much less poisoning to Pt-based catalysts. Although, the energy density of formic acid is lower than that of methanol, nevertheless, considering the fact that water is not necessary for the overall electrooxidation reaction of formic acid, a higher formic acid concentrations can be employed, and fuel cell can run more efficiently at higher voltages [6,7]. Literatures published about DFAFC gradually increased [1,5–10]. Only a small number of experimental impedance studies exist concerning formic acid electrooxidation on Pt/C and PtPd/C catalysts in $HClO_4$ [4] and polycrystalline Pt wire electrodes [11,12]. At present the investigation about electrochemical impedance spectroscopy (EIS) on Pt/C catalyst in H_2SO_4 medium is not explored yet.

The research with conventional electrochemical methods showed that the catalytic activity of the Pt/C catalyst (Johnson Matthery Inc.) with an average particle size of 2.5 nm for formic acid electrooxidation was much higher than that for methanol electrooxidation in this paper. The Pt/C catalyst for electrooxidation of methanol and formic acid was characterized and compared by using EIS technique combined with CV. The mechanisms of formic acid electrooxidation on Pt/C catalyst were also explored.

2. Experimental

2.1. Chemicals

All chemicals were analytically pure and used as received. Pt/C catalyst with an average particle size of 2.5 nm was bought from Johnson Matthery Inc.

2.2. Preparation of working electrode and its electrochemical measurements

2.2.1. Preparation of working electrode

Glassy carbon working electrode, 3 mm in diameter (electrode apparent area 0.0706 cm^2), polished with 0.05 μm alumina to a mirror-finish before each experiment, was used as substrate for the carbon-supported catalyst. For the electrode preparation, 5 μL of an ultrasonically redispersed catalyst suspension was pipetted

* Corresponding author. Tel.: +86 451 86417853; fax: +86 451 86413707.
E-mail address: wangzhenbo1008@yahoo.com.cn (Z.-B. Wang).

0378-7753/$ – see front matter © 2009 Elsevier B.V. All rights reserved.
doi:10.1016/j.jpowsour.2009.01.008

onto the glassy carbon substrate. After the solvent evaporation, the deposited catalyst (28 $\mu g_{metal}\ cm^{-2}$) was covered with 5 μL of a dilute aqueous Nafion® solution (5 wt.%). The resulting Nafion® film with a thickness of ≤0.2 μm had a sufficient strength to attach the carbon particles permanently to the glassy carbon electrode without producing film diffusion resistances [13,14]. The Faradic impedance of the thin film electrode was measured without mass transport limitations in order to investigate the kinetics and the mechanisms of electrooxidation of methanol and formic acid.

2.2.2. Electrochemical measurements

Electrochemical measurements were carried out with a conventional sealed three-electrode electrochemical cell at 25 °C. The glassy carbon thin film electrode as the working electrode was covered with the Pt/C catalyst powder. A piece of Pt foil of 1 cm^2 area was used as the counter one. The reversible hydrogen electrode (RHE) was used as the reference one with its solution connected to the working electrode by a Luggin capillary whose tip was placed appropriately close to the working electrode. All potential values are vs. RHE. All the solutions were prepared with ultrapure water (MilliQ, Millipore, 18.2 MΩ cm). Solutions of 0.5 mol L^{-1} H_2SO_4 containing 0.5 mol L^{-1} CH_3OH and 0.5 mol L^{-1} H_2SO_4 containing 0.5 mol L^{-1} HCOOH were stirred constantly and purged with ultrapure argon gas, respectively. Electrochemical experiments were performed by using a CHI650C electrochemical analysis instrument. Cyclic voltammogram (CV) was plotted within a potential range from 50 mV to 1200 mV with scanning rates of 1 mV s^{-1} and 20 mV s^{-1}, respectively. The potential of amperometric $i-t$ experiments jumped from 100 mV to 500 mV. EIS were usually obtained at frequencies between 0.01 Hz and 100 kHz with 12 points per decade. The amplitude of the sinusoidal potential signal was 5 mV. Due to a slight contamination from the Nafion® film, the working electrodes were electrochemically cleaned by continuous cycling at 50 mV s^{-1} until a stable response was obtained before the measurement curves were recorded.

3. Results and discussion

3.1. Electrochemical activity of Pt/C for electrooxidation of methanol and formic acid

Fig. 1 shows that CV curves for electrooxidation of methanol and formic acid on Pt/C catalyst with a scan rate of 20 mV s^{-1}. The CV

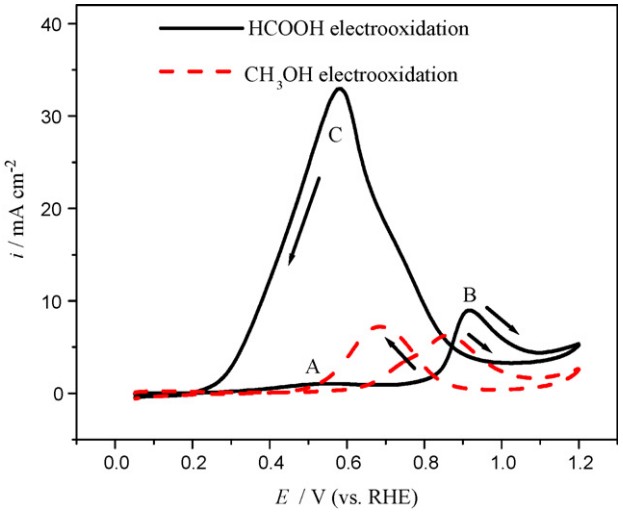

Fig. 1. Cyclic voltammetry curves of electrooxidation of methanol and formic acid on the Pt/C catalyst in the Ar-saturated solutions of 0.5 mol L^{-1} H_2SO_4 containing 0.5 mol L^{-1} CH_3OH and 0.5 mol L^{-1} H_2SO_4 containing 0.5 mol L^{-1} HCOOH at 25 °C. Scan rate: 20 mV s^{-1}.

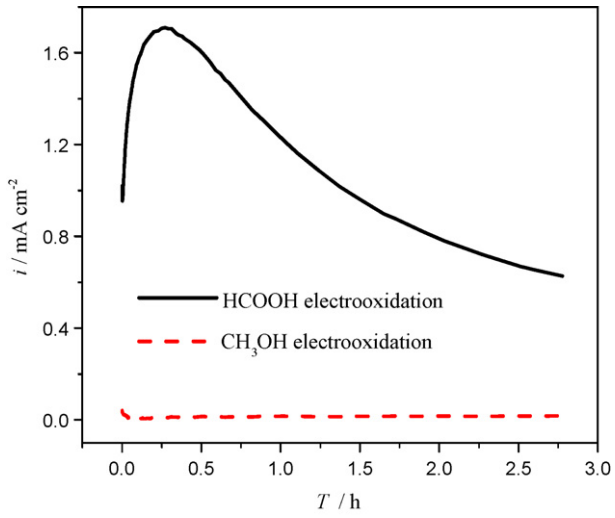

Fig. 2. Amperometric $i-t$ curves of electrooxidation methanol and formic acid on the Pt/C catalyst in the Ar-saturated solutions of 0.5 mol L^{-1} H_2SO_4 containing 0.5 mol L^{-1} CH_3OH and 0.5 mol L^{-1} H_2SO_4 containing 0.5 mol L^{-1} HCOOH at 25 °C at a fixed potential of 500 mV.

curve for methanol electrooxidation presents typical profile characterized by the inhibition of hydrogen adsorption/desorption region as shown by dashed. Its onset peak potential and peak potential are about 600 mV and 850 mV, respectively, during the positive scan. In the negative scan, the current presents an increase starting at 880 mV with a peak at about 680 mV, and then falling to zero at potentials below 500 mV. The hydrogen adsorption/desorption peaks on Pt/C catalyst are evidently inhibited from 50 mV to 500 mV due to methanol adsorption. Two peaks are observed in the positive scan at about 550 mV (peak A) and 920 mV (peak B) in CV curve for formic acid electrooxidation as shown by solid line in Fig. 1. Only one peak at 580 mV (peaks C) is observed during the negative scan. As we known, HCOOH electrooxidation on platinum electrode has CO_2 [15,16] as main product and CO_{ads} as predominant byproduct [17–19]. Similar to CH_3OH electrooxidation process, the hydrogen adsorption/desorption peaks are suppressed from 50 mV to 400 mV. The first small anodic peak about 550 mV (peaks A) is ascribed to the direct electrooxidation of HCOOH to CO_2 in the Pt surface active sites that remained unblocked after intermediate CO_{ads} adsorption [20,21]. The second anodic peak is related to the CO_{ads} oxidation, which releases the Pt surface active sites for the subsequent direct electrooxidation of HCOOH molecules. On the negative scan, a large cathodic peak that presents the real catalytic activity of the Pt surface is observed, as most of the surface active sites are free from occupation by the CO_{ads} and oxide species, and thus available for the formic acid electrooxidation [17]. Compared with that of 6.2 mA cm^{-2} for methanol electrooxidation during anodic scan, the activity of Pt/C catalyst for formic acid electrooxidation is very high with a current peak of 33.0 mA cm^{-2} at cathodic peak (peak C) that presents the real catalytic activity of the Pt surface [1,15].

The activity and stability of anodic catalysts can be evaluated with the steady-state current densities on the amperometric $i-t$ curves of electrooxidation of methanol and formic acid as shown in Fig. 2, which are the results of measurements in the Ar-saturated solutions of 0.5 mol L^{-1} H_2SO_4 containing 0.5 mol L^{-1} CH_3OH and 0.5 mol L^{-1} H_2SO_4 containing 0.5 mol L^{-1} HCOOH on a constant potential jump from 100 mV to 500 mV at 25 °C. Compared with that (0.018 mA cm^{-2} at 10,000 s) for methanol electrooxidation on Pt/C catalyst at the same potentials, the higher current density (0.63 mA cm^{-2} at 10,000 s) indicates the superior activity and

stability for formic acid electrooxidation on the Pt/C, which is consistent with the result of cyclic voltammetry.

3.2. Impedance patterns of formic acid electrooxidation on the Pt/C catalyst

In this section, the EIS technique was used to test the catalytic activity for formic acid electrooxidation on Pt/C catalyst. The EIS (A) and the phase shift (B) of formic acid electrooxidation on Pt/C catalyst at different potentials are shown in Fig. 3. The EIS results indicate that formic acid electrooxidation on Pt/C catalyst at various potentials shows almost the same impedance behavior, namely, there is only one arc in the 2nd and 3rd quadrants, and its diameter decreases evidently with the increase of the potential. The absolutely opposite impedance trends were observed on polycrystalline Pt wire electrodes [11,12], Pt/C thin film electrode [22], Pt–Sn anode [23], and Pt–Ru–Ni [24] for methanol electrooxidation, and polymer electrolyte membrane fuel cells for H_2/CO electrooxidation [25,26]. The results are also different with those on Pt/C and PtPd/C catalysts in $HClO_4$ medium [4]. Those differences should be attributed to the different use of catalysts and/or media and various measurement conditions. A large arc as shown in Fig. 3A reveals a slow reaction rate of formic acid electrooxidation. It is understood that the slow

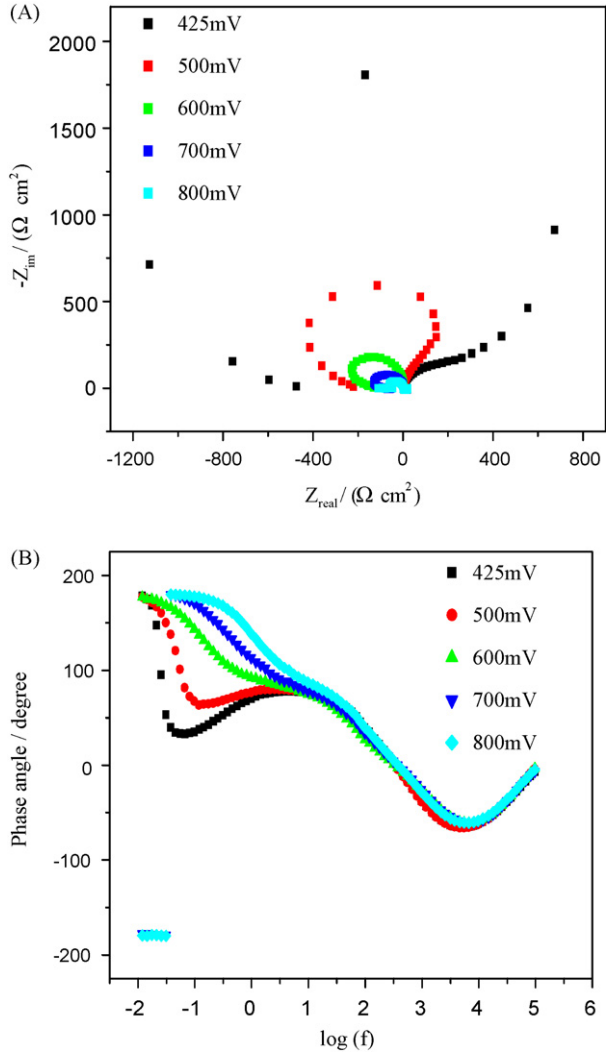

Fig. 3. Impedance patterns (A) and phase shift plots (B) of formic acid electrooxidation in an Ar-saturated solution of 0.5 mol L^{-1} HCOOH and 0.5 mol L^{-1} H_2SO_4 at 25 °C on Pt/C catalyst at different polarization potentials.

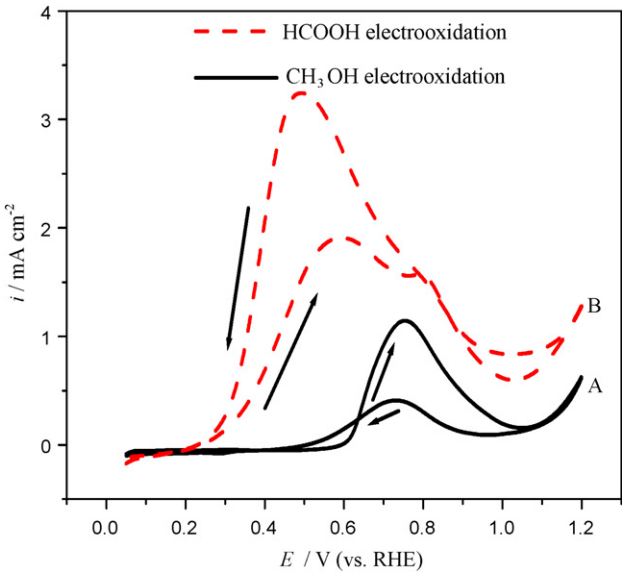

Fig. 4. Cyclic voltammetry curves of electrooxidation of methanol and formic acid on Pt/C catalyst in the Ar-saturated solutions of 0.5 mol L^{-1} H_2SO_4 containing 0.5 mol L^{-1} HCOOH and 0.5 mol L^{-1} H_2SO_4 containing 0.5 mol L^{-1} CH_3OH at 25 °C. Scan rate: 1 mV s^{-1}.

kinetics is caused by the direct electrooxidation of HCOOH to CO_2 in the Pt surface active sites that remained unblocked after intermediate CO_{ads} adsorption [7,17,27]. With the increase of the potential, the diameter of arc decreases rapidly, indicating that the charge transfer resistances for formic acid electrooxidation decrease markedly with potentials. Only one U-type peak can be observed at low potentials (425 mV and 500 mV) as shown in Fig. 3B, indicating that only one reaction happens on the electrode surface, *i.e.*, formic acid dehydrogenation reaction. With the increase of the potential, the U-type peak decreases gradually and disappears, the peak shifts toward higher frequency regions. As potentials arrive at 700–800 mV, a sudden change of phase angle happens as shown in Fig. 3B. The two unattached positive and negative values of phase angle appear. The main reason is that the rate-determining step changes from formic acid electrooxidation removal to oxygen evolution.

Comparison of the impedance plots, CV curves with a scanning rate of 1 mV s^{-1} as shown in Fig. 4, and mechanism of formic acid electrooxidation, it indicates that the surface active sites of catalyst are mostly occupied by the adsorbed CO formed as one of the intermediates of formic acid electrooxidation and thus is small at low potentials (at 400–500 mV) [11]. The rate determining step of formic acid is electrooxidaton of adsorbed CO. With the continuous increase of the potential between 500 mV and 700 mV as shown in Fig. 3A, the rate determining step is direct electrooxidation of formic acid. An explanation for the occurrence of behavior during formic acid electrooxidation can be elucidated [11,27]: the active sites on platinum are covered initially with the CO_{ads} layer formed as one of the intermediates of formic acid dehydration, and thus deactivated at lower potentials. As potential increases, some of the weakly CO_{ads} begin to be oxidized, producing Pt active sites in the adsorbed CO layer. Subsequent formic acid molecules then can be adsorbed and oxidized in these active sites. Consequently, the reaction rate of formic acid electrooxidation is sharply increasing. Namely, the direct dehydrogenation mechanism of formic acid is dominant.

3.3. Comparison of impedance patterns for electrooxidation of formic acid and methanol on Pt/C catalyst

The impedance patterns of formic acid electrooxidation on the Pt/C catalyst are obviously different with those of methanol

electrooxidation at 500 mV, 600 mV, and 700 mV as shown in Figs. 5–7.

The Faradaic admittances (the inverse of the Faradaic impedance) of electrooxidation of methanol and formic acid are [28]:

$$Y_F = \frac{1}{R_{ct}} + \frac{B}{a + j\omega} \quad (1)$$

where $R_{ct} = (\partial E/\partial I_F)_{ss}$ is charge transfer resistance of the electrode reaction. Its value is always positive. The subscript "ss" stands for steady state. I_F denotes the Faraday current. It can be seen from Figs. 5–7 that the reaction resistances (R_{ct}) for formic acid electrooxidation on the Pt/C catalyst is smaller than for methanol electrooxidation at a potential of 500 mV, yet R_{ct} for formic acid electrooxidation is markedly bigger than for methanol electrooxidation at a potential of 600 mV, and then R_{ct} for formic acid electrooxidation is slightly bigger than for methanol electrooxidation at 700 mV. The direction of U-type peak in phase shift plot for formic acid electrooxidation at low frequency region is upwards and acute at a potential of 500 mV, and that for methanol electrooxidation is downwards and obtuse as shown in Fig. 5B. With the increase of the potential, the U-type peak for formic acid electrooxidation becomes obtuse, and that for methanol electrooxidation is much sharper at 600 mV. However, the directions of their U-type peaks do not change. Their locations only shift slightly. Their U-type peaks disappear, and the two unattached positive and negative values of phase angle appear at 700 mV as shown in Fig. 7B. Their forms are absolutely different.

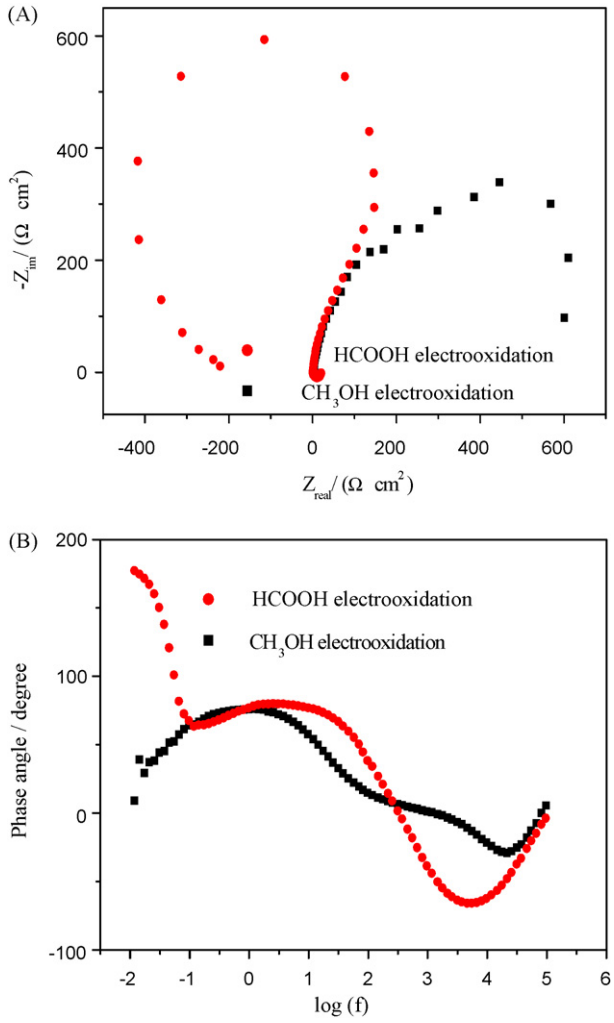

Fig. 5. Impedance patterns (A) and phase shift plots (B) of electrooxidation of methanol and formic acid in the Ar-saturated solutions of 0.5 mol L^{-1} H_2SO_4 containing 0.5 mol L^{-1} CH_3OH and 0.5 mol L^{-1} H_2SO_4 containing 0.5 mol L^{-1} HCOOH at 25 °C on Pt/C catalyst at 500 mV.

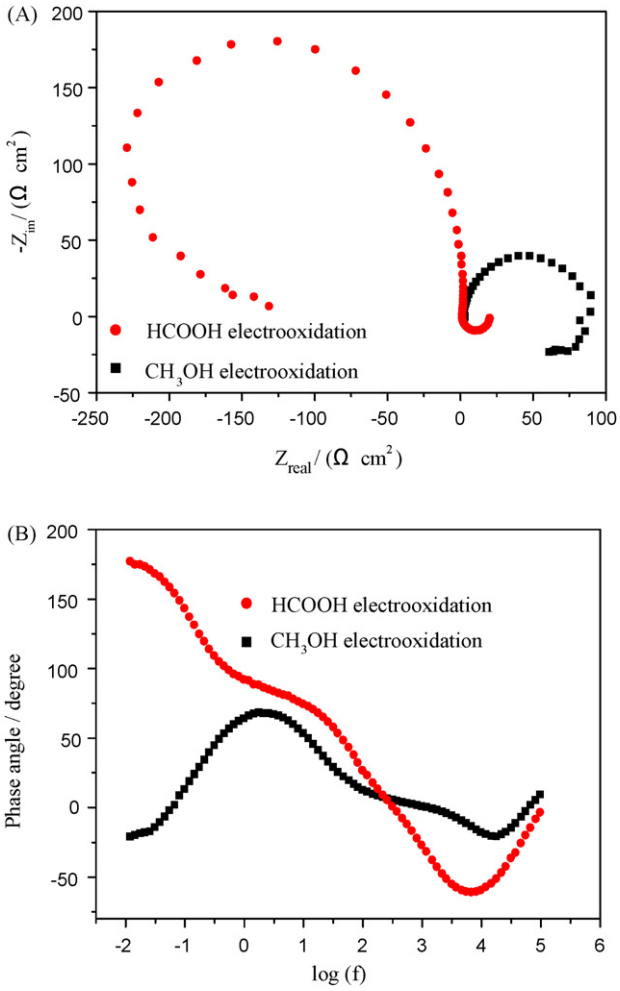

Fig. 6. Impedance patterns (A) and phase shift plots (B) of electrooxidation of methanol and formic acid in the Ar-saturated solutions of 0.5 mol L^{-1} H_2SO_4 containing 0.5 mol L^{-1} CH_3OH and 0.5 mol L^{-1} H_2SO_4 containing 0.5 mol L^{-1} HCOOH at 25 °C on Pt/C catalyst at 600 mV.

It is easy to understand for those phenomena: the rate determining steps are the methanol dehydrogenation forming adsorbed CO and formic acid dehydrogenation forming the final product CO_2, respectively, at a potential of 500 mV. The reaction rate of methanol dehydrogenation is evidently slower than that of formic acid as shown in Fig. 5. The oxidation of adsorbed CO from methanol dehydrogenation becomes the rate determining step due to favoring OH species formation on Pt/C at 600 mV. However, the rate determining step for formic acid electrooxidaton is the dehydration of formic acid at this potential, which is slightly slower than that of adsorbed CO as shown in Fig. 6. As the potential reaches 700 mV, due to the surface active sites of catalyst are covered by the OH_{ads}, the adsorption and oxidation rates of the methanol and formic acid molecules get slow and difficult as shown in Fig. 7. Within the potential range of interest for fuel cell, the activity of formic acid electrooxidation on Pt/C catalyst is prominently higher than that of methanol electrooxidation.

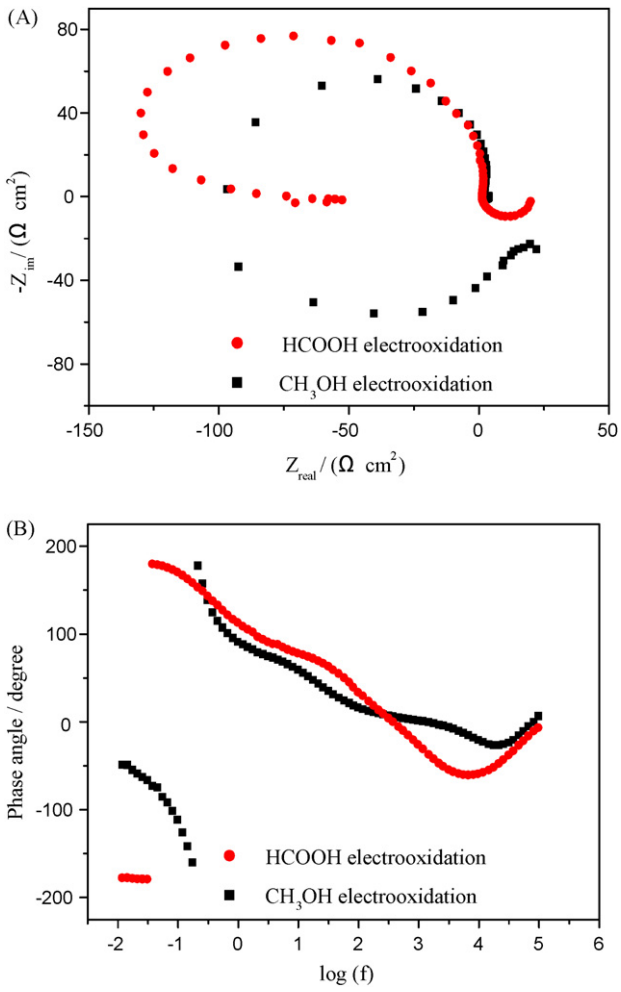

Fig. 7. Impedance patterns (A) and phase shift plots (B) of electrooxidation of methanol and formic acid in the Ar-saturated solutions of 0.5 mol L^{-1} H_2SO_4 containing 0.5 mol L^{-1} CH_3OH and 0.5 mol L^{-1} H_2SO_4 containing 0.5 mol L^{-1} HCOOH at 25 °C on Pt/C catalyst at 700 mV.

4. Conclusions

Electrocatalytic activities of the Pt/C catalyst for formic acid and methanol were investigated by the EIS combined with the conventional electrochemical methods in H_2SO_4 solution. The electrooxidation of methanol and formic acid on the Pt/C catalyst at various potentials shows absolutely different impedance behaviors. The rate determining step of formic acid electrooxidation is its dehydrogenation forming the final product CO_2 at 500 mV. With the potential range of interest for fuel cell, the rate of formic acid electrooxidation on Pt/C catalyst is prominently higher than that of methanol electrooxidation. The results of EIS measurement, which the electrooxidaton rates of formic acid and methanol were compared, were consistent with those of the conventional electrochemical methods.

Acknowledgments

This research is financially supported by the National Natural Science Foundation of China (Grant No. 20606007), the Scientific Research Foundation for the Returned Overseas Chinese Scholars, State Education Ministry (2008), Scientific Research Foundation for Returned Scholars of Heilongjiang Province of China (LC08C33), Postdoctoral Science-Research Developmental Foundation of Heilongjiang Province of China (LBH-Q07044), and Harbin Innovation Science Foundation for Youths (2007RFQXG042).

References

[1] C. Rice, S. Ha, R.I. Masel, P. Waszczuk, A. Wieckowski, Tom Barnard, J. Power Sources 111 (2002) 83–89.
[2] R. Chen, T.S. Zhao, J. Power Sources 167 (2007) 455–460.
[3] Z.X. Liang, T.S. Zhao, J. Phys. Chem. C 111 (2007) 8128–8134.
[4] X. Wang, J.M. Hu, I.M. Hsing, J. Electroanal. Chem. 562 (2004) 73–80.
[5] J.B. Xu, T.S. Zhao, Z.X. Liang, J. Power Sources 185 (2008) 857–861.
[6] M. Weber, J.T. Wang, S. Wasmus, R.F. Savinell, J. Electrochem. Soc. 143 (1996) L158–L160.
[7] S.J. Kang, J. Lee, J.K. Lee, S.Y. Chung, Y. Tak, J. Phys. Chem. B 110 (2006) 7270–7274.
[8] J. Yeom, R.S. Jayashree, C. Rastogi, M.A. Shannon, P.J.A. Kenis, J. Power Sources 160 (2006) 1058–1064.
[9] S. Uhm, S.T. Chung, J. Lee, Electrochem. Commun. 9 (2007) 2027–2031.
[10] J.H. Choi, K.J. Jeong, Y.J. Dong, J. Han, T.H. Lim, J.S. Lee, Y.E. Sung, J. Power Sources 163 (2006) 71–75.
[11] F. Seland, R. Tunold, D.A. Harrington, Electrochim. Acta 53 (2008) 6851–6864.
[12] H. Matsui, M. Yasuzawa, A. Kunugi, Electrochim. Acta 38 (1993) 1899–1901.
[13] T.J. Schmidt, H.A. Gasteiger, G.D. Stab, P.M. Urban, D.M. Kolb, R.J. Behm, J. Electrochem. Soc. 145 (1998) 2354–2358.
[14] Z.B. Wang, G.P. Yin, P.F. Shi, J. Electrochem. Soc. 152 (2005) A2406–A2412.
[15] S.G. Lemos, R.T.S. Oliveira, M.C. Santos, P.A.P. Nascente, L.O.S. Bulhoes, E.C. Pereira, J. Power Sources 163 (2007) 695–701.
[16] S. Wasmus, W. Vielstich, Electrochim. Acta 38 (1993) 185–189.
[17] J.D. Lovic, A.V. Tripkovic, S.Lj. Gojkovic, K.Dj. Popovic, D.V. Tripkovic, P. Olszewski, A. Kowal, J. Electroanal. Chem. 581 (2005) 294–302.
[18] G.Q. Lu, A. Crown, A. Wieckowski, J. Phys. Chem. B 103 (1999) 9700–9711.
[19] V. Selvaraj, M. Alagar, I. Hamerton, Appl. Catal. B: Environ. 73 (2007) 172–179.
[20] T. Iwastita, J. Braz. Chem. Soc. 13 (2002) 401–409.
[21] A. Capon, R. Parsons, J. Electroanal. Chem. 44 (1973) 239–254.
[22] I.M. Hsing, X. Wang, Y.J. Leng, J. Electrochem. Soc. 149 (2002) A615–A621.
[23] F. Matsumoto, C. Roychowdhury, F.J. DiSalvo, H.D. Abruña, J. Electrochem. Soc. 155 (2008) B148–B154.
[24] Z.B. Wang, G.P. Yin, Y.Y. Shao, B.Q. Yang, P.F. Shi, P.X. Feng, J. Power Sources 165 (2007) 9–15.
[25] N. Wagner, E. Gülzow, J. Power Sources 127 (2004) 341–347.
[26] M. Ciureanu, H. Wang, J. Electrochem. Soc. 146 (1999) 4031–4040.
[27] J.M.A. Harmsen, L. Jelemensky, P.J.M.V. Andel-Scheffer, B.F.M. Kuster, G.B. Marin, Appl. Catal. A: Gen. 165 (1997) 499–509.
[28] G. Wu, L. Li, B.Q. Xu, Electrochim. Acta 50 (2004) 1–10.